Frost Damage Progression Studied Through X-Ray tomography In Mortar With Phase Change Materials

Romero Rodriguez, Claudia; Chaves Figueiredo, Stefan; França de Mendonça Filho, Fernando; Schlangen, E.; Šavija, Branko

DOI
10.21012/FC10.235085

Publication date
2019

Document Version
Final published version

Published in
Proceedings of the 10th International Conference on Fracture Mechanics of Concrete and Concrete Structures

10^{th} International Conference on Fracture Mechanics of Concrete and Concrete Structures
FraMCoS-X
G. Pijaudier-Cabot, P. Grassl and C. La Borderie (Eds)
https://doi.org/10.21012/FC10.235085

FROST DAMAGE PROGRESSION STUDIED THROUGH X-RAY TOMOGRAPHY IN MORTAR WITH PHASE CHANGE MATERIALS

CLAUDIA ROMERO RODRIGUEZ*, STEFAN CHAVES FIGUEIREDO, FERNANDO FRANCA DE MENDONCA FILHO, ERIK SCHLANGEN AND BRANKO ŠAVIJA

* Delft University of Technology
Delft, the Netherlands
e-mail: c.romerorodriguez@tudelft.nl

Key words: Frost salt-scaling, phase change materials, freeze-thaw damage, durability

Abstract. The potential of using phase change materials (PCM) in cementitious materials to mitigate damage due to thermal loadings has been recently focus of intensive research. In the case of PCM with transition temperatures near to the freezing point of water, their potential to delay frost in a cementitious matrix has been largely investigated through the monitoring of internal temperature changes when exposed to repeated cycles of subzero and ambient temperature. Yet, the effect of these admixtures to prevent damage in cement-based materials has not been directly studied. In this paper, mortars cylinders of two different sizes and containing 0, 10 and 30% of PCM replacement by volume of aggregates were subjected to frost salt scaling during freeze and thaw cycles. Prior to the start of the weathering and after cycles 1, 3, 7 and 15 the cylindrical specimens were subjected to X-ray microtomography to monitor morphological changes due to frost action, such as chipping and cracks. Compressive and flexural strength, coefficient of thermal expansion and apparent porosity of the undamaged composites were also investigated. Results suggest that the improvement of frost scaling resistance of the mortars with incorporated PCM is a trade-off between resulting mechanical properties, thermal volume stability and porosity of the composite, as evinced from the better performance of mortars with 10% of PCM replacement.

1 INTRODUCTION

In countries with temperate climate the susceptibility of concrete to degradation increases due to the fluctuation of subzero and positive temperatures during winter. Frost damage acts as accelerator to other deterioration processes in the material due to the presence of cracks and increased porosity [1].

Current practices to prevent frost deterioration in concrete elements are prescriptive-like and rely on the minimization of frost risk, such as the use of low water-to-cement ratios [2]. Frost resistant concretes have been proposed based on the approach of creating a uniform macropore system to promote ice nucleation and growth in such defects, capable of withstanding the pressures of crystallization. Some examples are the use of air-entrainment [3] and SAP admixtures [4].

A novel method for mitigating damage due to frost is the use of microencapsulated phase change materials (PCM) [5, 6]. Some types of PCM solidify at temperatures just above $0^{\circ}\ C$ while at the same time releasing latent heat to the surroundings (the concrete). When temperatures rise again, the PCM melt while storing a great deal of energy which can be released as heat when the temperatures decrease again and so on. Studies have shown the potential of PCM on delaying the achievement of subcooling temperatures and (allegedly) the onset of ice formation in the pores of cement-based materials [7].

In this study we look at the direct effects of PCM on frost salt-scaling resistance of mortar samples. Mortars with two different contents of PCM were compared to a reference mortar. First, the composites were characterized with regards to their apparent porosity and coefficient of thermal expansion, as well as to the their mechanical strength, namely compressive and flexural. Secondly, the studied mortars were exposed to freezing/thawing cycles aimed to accelerate the damage of the samples. Their relative length and surface scaling were measured after 1, 3 and 7 cycles. In parallel, the progressive damage during exposure, namely chipping and microcracking, was monitored through X-ray micro tomography. Characterization of the physical and mechanical properties of studied mortars show reduced mechanical properties and increased porosity and thermal expansion with increasing contents of PCM. Results relative to exposed samples show that whereas the frost resistance of the mortars is improved by the presence of PCM in low quantities, drawbacks of the inclusion of soft admixtures pay a toll when higher levels of additions are used.

2 EXPERIMENTAL METHODOLOGY

2.1 Raw materials and sample preparation

Mortar samples were produced with cement CEM I 42.5N from ENCI Netherlands, tap water, superplasticizer Master Glenium 51 from BASF, standard quartz sand 0.08/2 mm from Normensand and encapsulated phase change material from Encapsys. The PCM used in this study presented a transition temperature range between $-16°C$ and $4°C$. Latent heat of fusion was found to be $131.27\ J/g$ from heat flow measurements via differential scanning calorimetry (DSC) using a DSC 8500 from PerkinElmer. The raw PCM were heated and cooled between $-20\ °C$ and $100\ °C$ at a rate of $5\ °C/min$. The microcapsules presented spherical appearance and diameters in the range. Mix designs of the studied mortars can be found in Table I.

TABLE I: *Mix design of mortars with 0, 10 and 30 % PCM by volume of cement paste.*

Mix.	CemI 42.5N	Sand 0.08/2 mm	PCM	Wat.	Sp
REF	514	1542	0	257	0.22
PCM10	514	1428.2	38.6	257	0.44
PCM30	514	1200.3	115.7	257	1

Cast samples were stored at laboratory conditions for 24 hours prior to demoulding. Subsequently, the samples were stored in a curing room at a temperature of $20\ (\pm 1)\ °C$ and a relative humidity of $95\ \%$.

2.2 Test methods and samples

After 28 days of curing, apparent porosity was measured on cylindrical samples with diameter of 35 mm and height of 70 mm. The samples were first vacuum saturated for 24 hours and their weight measured in air (m_s) and hydrostatically (m_h). They were then dried in an oven at $105\ °C$ until constant mass attainment (m_d). The apparent porosity was calculated as in Equation 1.

$$\phi = \frac{m_s - m_d}{m_s - m_h} \tag{1}$$

The coefficient of thermal expansion of 56 days old sealed mortars was measured in a range of 10 to $50\ °C$ by means of linear variable differential transformers (LVDT). The samples, with dimensions $40 \times 40 \times 160\ mm$, were preconditioned in an oven at $40\ °C$ for 14 days prior to the test to promote an even moisture distribution.

Flexural strength was measured in three-point-bending configuration in $40 \times 40 \times 160\ mm$ prims with a rate of $0.5\ kN/s$. The resulting halves were then tested in compression at a rate of $13.5\ kN/s$. A servo-hydraulic press was used for the tests.

At age 28 days three prismas per mortar type were insulated with styrofoam from all surfaces minus the top (coincident with the troweled surface). The exposed surface, laying on two rods perpendicular to the span of the beam, was put in contact with a 3 % NaCl solution from below (see scheme in Figure 1. After 24 hours of chlorides ingress promotion, 7 freezing/thawing cycles were run. Each cycle consisted of 16 hours of exposure at $-21°C$ and 8 hours at $21°C$. Such harsh cycle settings were chosen in order to accelerate the damage in the samples rather than to simulate realistic frost exposure of concrete elements [8].

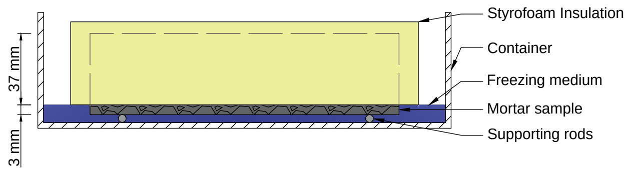

Figure 1: Scheme of frost salt-scaling exposure.

Relative length change and mass scaling were measured after 1, 3 and 7 freezing/thawing cycles according to [9, 10].

2.3 X-ray micro tomography

Mortar cylinders with diameters 25 mm and height of 30 mm were used to monitor the progressive damage due to frost action through X-ray microtomography. The samples were insulated in the same way as shown for the beam samples described in the previous section. The scans were acquired after 1, 3, 7 and 14 freeze/thaw cycles. A Micro CT-Scanner (Phoenix Nanotom, Boston, MA, USA) was used. The X-ray tube was operated at 120 kV and 60 μA. 2800 projections with an exposure of 6 s were acquired by a digital GE DXR detector (3072 $\times$ 2400 pixels). In order to minimize noise an average of 4 radiographs was done for each projection. The voxel resolution under these conditions resulted 11 μm. The 3D reconstruction of the acquired projections was carried out with the software VG Studio Max after calibration of the projections with dark and bright field images. Ring, spot and beam hardening artifacts were corrected during the reconstruction. In order to study the progressive damage of a single sample, the reconstructed scans carried out at different times during exposure were registered through the opensource software DataViewer from Bruker. Image analysis was then carried out through the freeware ImageJ.

3 RESULTS

3.1 Physical and mechanical characterization of mortars

A summary of the physical and mechanical properties of the investigated mortars is shown in Table II.

TABLE II: *Porosity (ϕ), coefficient of thermal expansion (α), compressive and flexural strength (f_c, f_{ct}) of mortars with 0, 10 and 30 % PCM by volume of cement paste.*

Mixture	ϕ [-]	α [$\mu m/m$]	f_c [MPa]	f_{ct} [MPa]
REF	0.177	12.1	41.7	8.5
PCM10	0.205	13.3	27.7	6.5
PCM30	0.24	16.3	19.5	5.7

The porosity accessible to water of the studied mortars does not provide a pore size distribution but the total open porosity including micro, meso and macro pores. Also, drying of the mortars at 105 $°C$, may result in a coarsened pore structure. Therefore, these values should be not be taken as absolute. The values for REF, PCM10 and PCM30 were found to be 17.7 %, 20.5 % and 24 %, respectively. Mortar REF presents the lowest volume of open porosity. PCM30 shows a relevant increase in porosity of around 37 % with respect to the reference mortar whereas the porosity of PCM10 increases only of a 15 %. These results seem to indicate that the replacement of sand volume by PCM microcapsules influences strongly the pore structure of the mortars. In a study from [11], the authors indicate that PCM microcapsules promote nucleation of reaction products and therefore the phases assemblage in the hydrated matrix changed. A second explanation may come from the increase in specific surface of the interfacial transition zone (ITZ) due to the replacement of aggregates with variegated dimensions ranging from 0.08 to 2 mm by microcapsules.

The inclusion of PCM also resulted in changes in the coefficient of thermal expansion of the composites. Namely, the coefficient of thermal expansion increased when larger replacement of PCM were used. This does not come by surprise since quartz aggregates present a better thermal stability [12] than the soft PCM microcapsules.

Regarding the mechanical strength, as reported also elsewhere [13], higher leves of replacement result in dramatic decreases of the compressive strength, halved when 30 % of PCM are added, and moderated decreases of flexural strength. A possible cause for these decreases in this study is the fact that part of the quartz aggregates, with high mechanical strength, was substituted with soft inclusions, which offer little mechanical resistance. In a study performed by [14] the authors suggest that the PCM-associated ITZ significantly decreases the stiffness of the composite. Other studies attribute the loss of strength to the breakage of the capsules during mixing and the interaction of the leaked PCM with the cement during hydration which might modify the hydration products and/or result in increased porosity [15]. Furthermore, the breakage of the capsules was shown in [16] to result on the agglomeration of PCM from more capsules which may have caused the presence of numerous weak zones.

3.2 Frost salt scaling damage

3.2.1 Standard tests

In Figure 2, the relative length change and the mass scaling of the weathered samples are displayed as a function of the number of cycles, respectively.

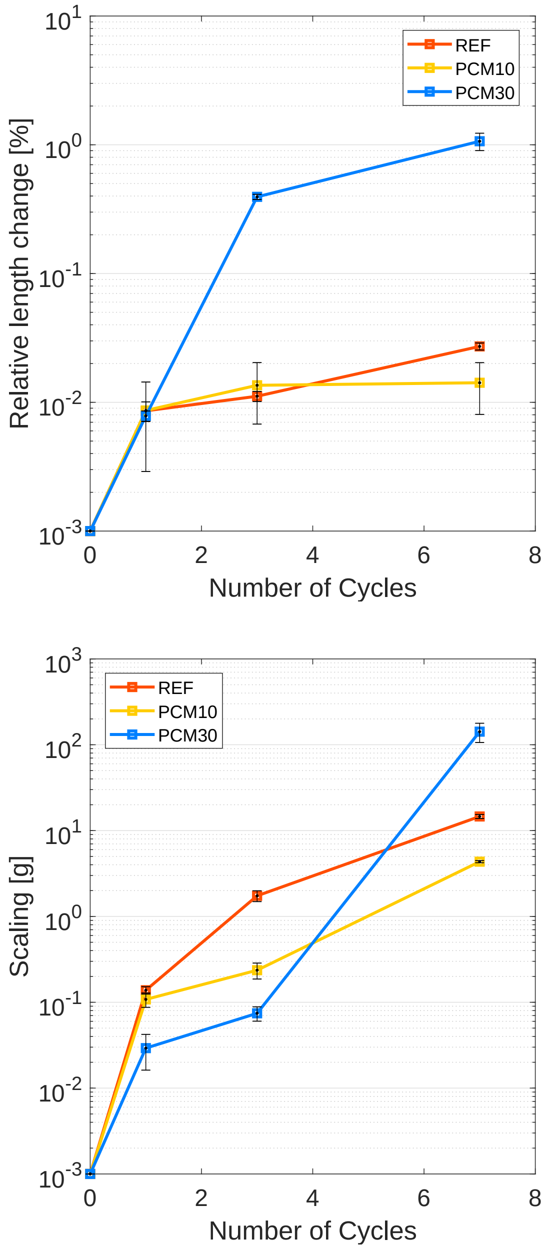

Figure 2: Relative length change a) and mass scaling b) of mortars REF, PCM10 and PCM30 during freeze and thaw cycles.

Relative length change of cementitious samples exposed to freezing and thawing conditioning is a simple way of measuring the internal damage present in the specimens. After cycle 1 almost no differences could be discerned between the different mortars, except for the high variability in length change for mortar PCM10. After the third cycle the length changes for REF and PCM10 kept being similar. However the length change read for PCM30 samples was one order of magnitude higher. After 7 cycles, the length change of PCM10 barely changed to $0.0142\ \%$, whereas REF samples showed an increased length change to $0.0272\ \%$. PCM30 showed an increased length change of $1.065\ \%$, two orders of magnitude higher than the other two mortars. According to the aforementioned results , mortar with $30\ \%$ of PCM by volume of cement paste presented the highest degree of damage at the end of the test, followed by the reference mortar. It seems that mortar with $10\ \%$ of PCM presented the least internal damage.

Frost salt scaling can be most simply assessed through the measurement of the scaled mass at the surface of conditioned samples. Scaling of the surface occurred as early as after the first cycle for all the mortars. Reference mortar presented the most scaling $0.14\ g$, followed very closely by the mortar with $10\ \%$ PCM by volume of cement paste with $0.11\ g$. PCM30 on the other hand showed almost no scaling with only $0.03\ g$. Same trend was observed also after 3 cycles. Yet, after the seventh cycle the mortar containing $30\ \%$ PCM by volume of cement paste showed the most scaling $142\ g$ overtaking the reference mortar with $14\ g$ and the one with $10\ \%$ PCM with $4\ g$ by one order of magnitude.

3.2.2 Damage monitoring through X-ray micro tomography

In Figure 3 the difference in volume after 14 weathering cycles with respect to the initial state of the studied samples are shown. It can be immediately observed that scaling was present for all the samples after 14 cycles of accelerated exposure to frost damage. From the differential volume it was obvious that PCM10 presented the least damage, which happened to be present at the exposed surface along the edge. It is also possible to observe that for REF and PCM30 chipping of material and cracking occurred near to the sample edges both at the exposed surface and at the insulated one.

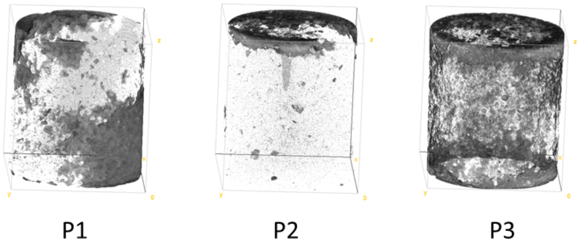

Figure 3: Substraction between scanned volume after 14 freezeing/thawing cycles and the initial volume for REF, PCM10 and PCM30 samples.

From the differential volumes the volume of cracks and chips of material were quantified per slice. In this way a spatial distribution of the damage was obtained. In Figure 4 vertical profiles of the damaged volume per slice are shown. The standardized height of the samples was used to account for the slight differences in absolute height among the studied samples.

First of all, it can be noticed that little to no damage for REF and PCM10 was observed at least up to after 3 cycles of freezing/thawing cycles, whereas PCM30 already exhibited some shallow chipping at the edges of the cylindrical sample. After 7 cycles REF and PCM30 started showing more frost damage. Specifically REF presented some damage along the first $5\ \%$ of the height from the surface exposed to the freezing medium, while PCM30 presented some $14\ \%$ of the height from the weathered surface and $4\ \%$ from the insulated one. Meanwhile PCM10 showed no sign of being affected by the weathering cycles, judging from the CT data. After 14 cycles, the harsh freezing/thawing cycles seemed to have affected all studied samples. The depth affected by the frost salt scaling from the exposed surface was 25, 12 and $31\ \%$ for REF, PCM10 and PCM30, respectively. The reference mortar and the mortar with $30\ \%$ PCM by volume of cement paste also presented damage within 60 and $13\ \%$ from the insulated surface, although somehow lower in volume than the damage present near to the weathered surface.

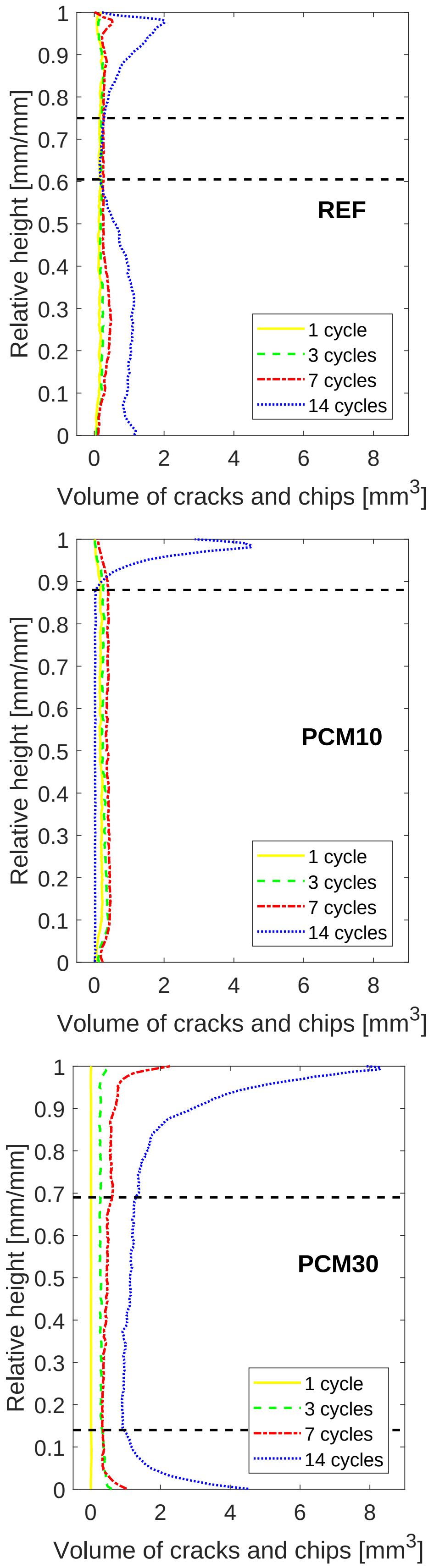

Figure 4: Cumulative volume of cracks and chips in studied mortars after 1, 3, 7 or 14 freezing/thawing cycles.

4 CONCLUSIONS

Based on the results presented in this study we can draw the following conclusions:

- The presence of PCM in mortar increases the coefficient of thermal expansion despite the evidence that higher porosity (in this case due to the addition of PCM) results in higher thermal stability of cementious materials [17]. According to the theory of glue-spalling [8], more compatible thermal expansion between the ice pool and the mortar might resultin increased resistance to frost salt-scaling.

- Compressive and flexural strength of mortars with PCM dramatically decrease when increasing dosages of PCM are used. Possible causes are the replacement of resistant aggregates with soft inclusions or the increase in specific surface area of ITZ. Lower tensile strength of the material might cause lower frost resistance of the composite.

- The replacement of aggregates with PCM inclusions results in increased porosity of the mortars which results in higher transport properties and therefore, increased water uptake.

- The replacement of aggregates with $10\ \%$ PCM by volume of cement paste improved the salt-scaling resistance of the mortar as evinced from standardized tests such as relative length change, mass scaling measurements and the assessment of crack volume from micro CT. Whereas, higher replacements like $30\ \%$ caused a dramatic decrease in frost resistance even with respect to the reference mortar.

ACKNOWLEDGEMENTS

This research was funded by the European Unions Seventh Framework Programme for research, technological development and demonstration under the ERA-NET Plus Infravation programme, grant agreement No.

31109806.0001. The first author acknowledges the financial support from the Construction Technology Research Program funded by the Ministry of Land, Infrastructure and Transport of the Korean Government under the grant 17SCIP-B103706-03. The authors would like to thank Encapsys, LLC, for providing the encapsulated PCMs.

REFERENCES

[1] Adam M Neville. *Properties of concrete*. Pearson Education India, 1963.

[2] BS EN. 206: 2013. *Concrete. Specification, performance, production and conformity*, 2013.

[3] Lianxiang Du and Kevin J Folliard. Mechanisms of air entrainment in concrete. *Cement and concrete research*, 35(8):1463–1471, 2005.

[4] Viktor Mechtcherine, Christof Schroefl, Mateusz Wyrzykowski, Michaela Gorges, Pietro Lura, Daniel Cusson, Jim Margeson, Nele De Belie, Didier Snoeck, Kazuo Ichimiya, et al. Effect of superabsorbent polymers (sap) on the freeze–thaw resistance of concrete: results of a rilem interlaboratory study. *Materials and Structures*, 50(1):14, 2017.

[5] Dale P Bentz and Randy Turpin. Potential applications of phase change materials in concrete technology. *Cement and Concrete Composites*, 29(7):527–532, 2007.

[6] A Sakulich and D Bentz. Limiting Freeze/Thaw Damage in Cementitious Infrastructure Systems with Phase Change Materials (PCMs). *Microscopy and Microanalysis*, 17(S2):1482–1483, July 2011.

[7] Jung Heum Yeon and Kwan-Kyu Kim. Potential applications of phase change materials to mitigate freeze-thaw deteriorations in concrete pavement. *Construction and Building Materials*, 177:202–209, July 2018.

[8] John J Valenza II and George W Scherer. A review of salt scaling: I. phenomenology. *Cement and Concrete Research*, 37(7):1007–1021, 2007.

[9] CEN/TR. 15177: 2006. *Testing the freeze-thaw resistance of concrete-Internal structural damage*, 2006.

[10] CEN/TS. 12390-9: 2016. *Testing hardened concrete - Part 9: Freeze-thaw resistance with de-icing salts - Scaling*, 2016.

[11] Amitha Jayalath, Rackel San Nicolas, Massoud Sofi, Robert Shanks, Tuan Ngo, Lu Aye, and Priyan Mendis. Properties of cementitious mortar and concrete containing micro-encapsulated phase change materials. *Construction and Building Materials*, 120:408–417, September 2016.

[12] DW Hobbs. The dependence of the bulk modulus, young's modulus, creep, shrinkage and thermal expansion of concrete upon aggregate volume concentration. *Matériaux et construction*, 4(2):107–114, 1971.

[13] Sandra Cunha, Marine Lima, and José B. Aguiar. Influence of adding phase change materials on the physical and mechanical properties of cement mortars. *Construction and Building Materials*, 127:1–10, November 2016.

[14] Gabriel Falzone, Guillermo Puerta Falla, Zhenhua Wei, Mingjie Zhao, Aditya Kumar, Mathieu Bauchy, Narayanan Neithalath, Laurent Pilon, and Gaurav Sant. The influences of soft and stiff inclusions on the mechanical properties of cementitious composites. *Cement and Concrete Composites*, 71:153–165, August 2016.

[15] Zhenhua Wei, Gabriel Falzone, Bu Wang, Alexander Thiele, Guillermo Puerta-Falla, Laurent Pilon, Narayanan Neithalath, and

Gaurav Sant. The durability of cementitious composites containing microencapsulated phase change materials. *Cement and Concrete Composites*, 81:66–76, 2017.

[16] Matthew Aguayo, Sumanta Das, Amit Maroli, Nihat Kabay, James C.E. Mertens, Subramaniam D. Rajan, Gaurav Sant, Nikhilesh Chawla, and Narayanan Neithalath. The influence of microencapsulated phase change material (PCM) characteristics on the microstructure and strength of cementitious composites: Experiments and finite element simulations. *Cement and Concrete Composites*, 73:29–41, October 2016.

[17] Qiang Zeng, Kefei Li, Teddy Fen-Chong, and Patrick Dangla. Effect of porosity on thermal expansion coefficient of cement pastes and mortars. *Construction and Building Materials*, 28(1):468–475, 2012.